

# Measurements of $H \rightarrow \tau\tau$ cross-section at FCC-ee

S. Giappichini<sup>●a</sup>, M. Klute<sup>●a</sup>, M. Presilla<sup>●a</sup>, X. Zuo<sup>●a,b</sup>, M. Cepeda<sup>c</sup>

<sup>a</sup>*Institute for Experimental Particle Physics (ETP), Karlsruhe Institute of Technology (KIT), Karlsruhe, Germany*

<sup>b</sup>*École Polytechnique Fédérale de Lausanne (EPFL), Lausanne, Switzerland*

<sup>c</sup>*Centro de Investigaciones Energéticas, Medioambientales y Tecnológicas (CIEMAT), Madrid, Spain*

## Abstract

The Future Circular Collider (FCC) stands at the forefront of the European Strategy for Particle Physics as the future flagship project at CERN. The  $H \rightarrow \tau\tau$  decay, featuring a large branching ratio, clean identification in the FCC-ee environment, and the possibility to reconstruct polarization information, is an excellent channel to measure Higgs properties. This work shows the expected precision for the  $H \rightarrow \tau\tau$  cross-section measurement at the FCC-ee in the ZH production mechanism at  $\sqrt{s} = 240$  GeV and  $\sqrt{s} = 365$  GeV, as well as via the vector boson fusion process at  $\sqrt{s} = 365$  GeV. Furthermore, we explore and evaluate a set of methods for reconstructing tau decays. These techniques are critical for unlocking the full physics potential of the FCC-ee and for improving the understanding of tau-related observables in both Standard Model measurements and New Physics searches. The results obtained significantly enhance the FCC-ee outlook in the  $H \rightarrow \tau\tau$  channel, improving it by at least an order of magnitude compared to the current sensitivity of measurements' performance at the LHC.

*Keywords:* Higgs physics, Future circular collider, Tau physics, Precision measurements

## 1. Introduction

After more than a decade of measurements at the LHC, Higgs couplings to Standard Model (SM) particles are now probed with percent-level precision across multiple production and decay channels, providing a unique window on the dynamics of the Electroweak Symmetry Breaking mechanism and possible new physics beyond the SM. In this context, precision studies of Higgs Yukawa interactions with charged leptons are especially powerful, since small deviations from the SM pattern can signal new degrees of freedom at higher scales. Among these, the  $H \rightarrow \tau\tau$  decay plays a central role: it is the most accessible leptonic Higgs decay mode at hadron colliders, with a relatively large branching fraction and a more favorable background environment compared to  $H \rightarrow b\bar{b}$ . The ATLAS and CMS Run I combination, obtained from proton-proton collisions at  $\sqrt{s} = 7$  and 8 GeV, marked the first observation of the  $H \rightarrow \tau\tau$  decay [1], while the first observation from a single experiment was obtained by the CMS experiment using data collected at a center-of-mass energy of 13 TeV [2].

The interest in the exploration of the Higgs sector with new dedicated colliders, alongside top and electroweak physics, has been recently formalized by the European Strategy for Particle Physics Update [3, 4, 5]. These machines offer a uniquely clean electron-positron collision environment, combining unprecedented luminosity with excellent signal-to-background ratios, and thereby enable major advances in precision measurements on comparatively short data-taking timescales.

The  $e^+e^-$  Future Circular Collider (FCC-ee) [6, 7] is

one of such proposed machines to be built at CERN in the coming years. The core of the FCC-ee program is to measure Higgs production inclusively [8, 9] with a dedicated run at  $\sqrt{s} = 240$  GeV, where about 2 million Higgs bosons would be produced in association with Z bosons (ZH) for an integrated luminosity of  $10.8 \text{ ab}^{-1}$ . Additionally, a run around the  $t\bar{t}$  threshold, at  $\sqrt{s} = 365$  GeV with an expected collected luminosity of  $3 \text{ ab}^{-1}$ , would also make accessible Higgs production from vector boson fusion (VBF). It would then be the first time that the Higgs boson is produced from  $e^+e^-$  collisions, allowing for model-independent measurements of its properties [10].

The main goal of this letter is to estimate the achievable relative uncertainty on the cross-section of the Higgs decay into a pair of taus in the ZH production channel at FCC-ee, at  $\sqrt{s} = 240$  GeV and  $\sqrt{s} = 365$  GeV, as well as from VBF at the top threshold, with the respective Feynman diagrams shown in Figure 1. The current measurements by the LHC experiments in these channels on the product  $\sigma \cdot BR(H \rightarrow \tau\tau)$ , normalized to the SM predictions, are respectively  $\mu_{ZH} = 1.89^{+0.65}_{-0.56}$  and  $\mu_{VBF} = 0.86^{+0.17}_{-0.16}$  from CMS [11], and  $\mu_{ZH} = 1.00^{+0.62}_{-0.59}$  and  $\mu_{VBF} = 1.00^{+0.21}_{-0.18}$  from ATLAS [12], where the signal strength  $\mu$  is defined as the ratio of the signal yield observed to that predicted by the SM. This results in approximately 60% relative uncertainty in the first channel and 20% in the second. The projections for HL-LHC, the next upgrade of the LHC with  $\mathcal{L}_{int} = 3 \text{ ab}^{-1}$  and  $\sqrt{s} = 14$  GeV, lower the value to 14% in the ZH channel and 4-8% in VBF [13, 14]. A different way to interpret the measurement is to consider the Higgs

coupling modifiers in the  $\kappa$  framework [15, 16], where  $\kappa_i$  parametrizes the measurable ratio of the Higgs coupling strength to particle  $i$  relative to the SM prediction. In this scheme, the current value for  $\kappa_\tau$ , which is related to the  $H \rightarrow \tau\tau$  vertex, is  $0.92 \pm 0.08$ , giving a relative precision of 8.6% from CMS [11], and  $0.93 \pm 0.07$  (7.5% precision) from ATLAS [12]. The corresponding estimation at HL-LHC improves the relative precision to 1.9% [17].

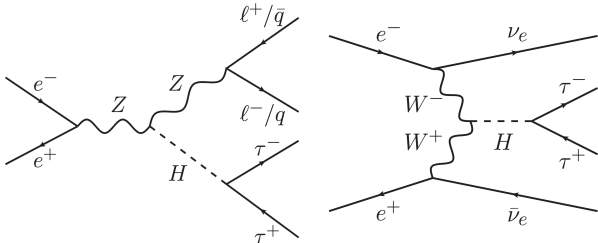


Figure 1: On the left: Feynman diagram for ZH events in  $e^+e^-$  collisions, where the Z boson decays to leptons (electrons or muons considered in this study), quarks or neutrino pairs, and the Higgs decays to a tau pair. On the right: Feynman diagram for VBF events (mediated by W bosons) in  $e^+e^-$  collisions, where the Higgs decays to a tau pair.

In the scope of this study, we also review and compare methods of tau reconstruction at future  $e^+e^-$  colliders, necessary to achieve high precision in the channel analyzed. Among the charged leptons, the tau remains the least precisely characterized, largely because of its numerous, predominantly hadronic decay modes, despite the Belle II collaboration recently reporting the most precise measurement of its mass [18]. It is expected that more than  $10^{11}$  tau pairs will be produced at FCC-ee, rivaling dedicated flavor factories, on account of the high luminosity achievable, and hadron colliders, where information loss is caused by the high event multiplicity. This would result in the improvement by several orders of magnitude of the current limits on tau observables [19, 20].

## 2. Event simulation and reconstruction

We use Monte Carlo (MC) samples for the signal and the SM backgrounds, simulated at Leading Order with different MC generators, including a parameterization of initial and final state radiation. The SM signals and all the relevant Higgs decays from ZH production ( $ZZ$ ,  $WW$ ,  $gg$ ,  $bb$ ,  $cc$ , and  $ss$ ), are generated with Whizard v. 3.0.3 [21, 22]. The same generator is used to simulate the Drell-Yan production to leptons,  $\gamma\gamma \rightarrow \ell\ell$ ,  $e\gamma \rightarrow eZ$  with Z decaying into electrons or muons, and  $ee \rightarrow \nu\nu Z$ . The hadronization of partons is simulated with Pythia6 [23]. The Drell-Yan to quarks,  $e^+e^- \rightarrow ZZ$ , and  $e^+e^- \rightarrow WW$ , are produced with Pythia8 [24]. For the  $\sqrt{s} = 365$  GeV analysis, the additional background coming from  $t\bar{t}$  is included and simulated with Pythia8.

A simulation of the IDEA detector concept [25], one of the main designs proposed for FCC-ee based on a short-

drift wire chamber and a dual-readout calorimeter, is performed. It relies on the fast-simulation package DELPHES v. 3.5.1pre05 [26]. The package FastJet [27] is used to cluster particles into jets with the  $e^+e^-$  exclusive Durham algorithm, setting  $n_{jets}$  equal to the expected number of jets in the events, as it best fits the clean environment of the collisions.

We divide the analysis into nine categories based on the decay of the Z bosons and the two taus, as well as the jet clustering algorithm used. The details are given in Table 1. In the VBF channel, the selection follows that of the  $Z \rightarrow \nu\nu$  channel.

Leptonic Z and tau decays ( $\tau_\ell$ ) are both identified directly from the isolated electrons and muons. To distinguish them in case of ambiguity, we first identify the opposite-sign, same-flavor lepton pair whose invariant mass is closest to the nominal Z boson mass and assign it to the Z candidate. The remaining leptons were then associated with the tau candidates.

Hadronic taus ( $\tau_h$ ) are constructed starting from jets with the procedure described in the following section, while also separating them from quark jets.

## 3. Tau reconstruction at the FCC-ee

This section compares two techniques for reconstructing hadronic tau decays at FCC-ee. In addition to their use in current cross-section measurements, these methods are broadly applicable to similar processes, such as  $Z \rightarrow \tau\tau$  events, and are crucial to maximizing the physics reach of future collider experiments. We examine a machine-learning-based approach and a method that explicitly assigns events to individual tau decay modes.

*ParticleNet reconstruction.* The ParticleNet algorithm [28], based on a graph neural network architecture for jet flavor identification, was previously trained on di-jet Higgs events for the FCC-ee [29] and offers the capability of individuating tau jets. In this case, tau jets are defined as having a tau score above 0.5, a criterion that quark jets do not meet. This value could be tuned in the future to achieve better purity at the expense of efficiency. The number of charged, neutral, and total constituents in the tau jets can be inferred, but it's less informative than a proper decay mode matching.

*Explicit reconstruction.* To identify the exact tau decay mode, a function is implemented to scan through the single jet constituents and identify the corresponding tau products. First of all, jets containing electrons or muons are immediately tagged as quark jets. For the remaining, the four-vector of the taus, along with the charge ( $\pm 1$ ) and mass (required to be smaller than 3 GeV), are based on the constituents spatially close ( $\Delta\theta < 0.2$ ) to the leading charged particle of the jet. The number of charged and neutral constituents is used to infer the tau decay mode, assigning a separate value to the rejected jets.

Table 2 shows the efficiency of both reconstruction methods, matching the reconstructed taus with the true

	$H \rightarrow \tau_h \tau_h$	$H \rightarrow \tau_\ell \tau_h$	$H \rightarrow \tau_\ell \tau_\ell$
$Z \rightarrow \ell\ell$	Exactly two leptons with same flavor and opposite signs are excluded from two jets	Exactly three leptons, two with opposite signs, are excluded from one jet	Exactly four leptons with total neutral charge and no hadrons, no clustering
$Z \rightarrow \nu\nu$	No leptons are present, two jets are clustered	Exactly one lepton excluded from one jet	Exactly two leptons with opposite sign and no hadrons, no clustering
$Z \rightarrow q\bar{q}$	Four jets from all particles	One isolated lepton with $p > 20$ GeV excluded from three jets	Two isolated leptons with $p > 20$ GeV excluded from two jets

Table 1: Definition of final object selection and clustering in each category of the analysis. Leptons,  $\ell$ , are either electrons or muons,  $q$  stands for all quarks except the top quark, and  $\nu$  includes all neutrino flavors.

ones. It is expected that the efficiency drops significantly when the  $Z$  decays hadronically, as these events are less clean, as well as for higher energies, where the two taus become collinear and thus more difficult to reconstruct in two separate jets. The efficiencies of the two methods are comparable, with a slight loss for the explicit reconstruction. The choice is then mainly motivated by the need to identify tau decay modes. In Figure 2, the confusion matrix for the true tau decay modes against the individuated ones is shown for the cases where the truth-matching was successful. This illustrates an almost perfect efficiency for all major decay modes. Separating further the ID by the number of neutral particles is found to be very inefficient due to the challenge of separating two or more photons in a small cone coming from the decay of neutral pions.

	ParticleNet		Explicit Reconstruction	
	240 GeV	365 GeV	240 GeV	365 GeV
$Z \rightarrow \nu\nu, H \rightarrow \tau\tau$	95.03%	93.67%	89.02%	88.80%
$Z \rightarrow ee, H \rightarrow \tau\tau$	86.69%	81.43%	86.35%	84.14%
$Z \rightarrow \mu\mu, H \rightarrow \tau\tau$	90.69%	87.17%	87.37%	85.95%
$Z \rightarrow bb, H \rightarrow \tau\tau$	61.78%	74.39%	77.69%	80.67%
$Z \rightarrow cc, H \rightarrow \tau\tau$	61.97%	74.24%	78.07%	80.96%
$Z \rightarrow ss, H \rightarrow \tau\tau$	61.87%	73.99%	78.45%	81.02%
$Z \rightarrow u\bar{u}/d\bar{d}, H \rightarrow \tau\tau$	61.98%	74.18%	78.32%	81.04%

Table 2: Efficiency of hadronic tau decay reconstruction with the ParticleNet algorithm and explicit reconstruction at  $\sqrt{s} = 240$  GeV and 365 GeV. The values correspond to matching the reconstructed tau to the generated one in a cone of  $\Delta R < 0.2$  rad.

Building on previous methods, electron-positron collisions make it possible to recover information about neutrinos in tau pairs with up to twofold ambiguity by considering the event's kinematics. However, some considerations need to be made. Firstly, either the center-of-mass of the di-tau system or the recoil system needs to be well known, meaning the missing energy in the event is exclusively related to the tau neutrinos. Secondly, the taus need to have enough separation to be reconstructed in two distinct jets. Finally, the tau mass is set a priori, and neutrinos are treated as massless particles. Examples can be found in Ref. [30, 31]. In this analysis, we do not exploit the full tau momentum information, as the previous methods already achieve good efficiency and separation with quark jets, so these methods are not going to be discussed further.

Since we are interested in studying the Higgs boson,

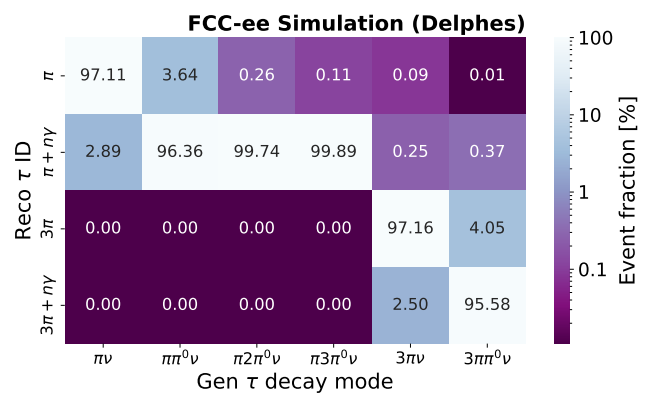


Figure 2: Confusion matrix of truth level tau decay modes against the ID from the explicit reconstruction method for  $Z \rightarrow \nu\nu$ ,  $H \rightarrow \tau\tau$  events at  $\sqrt{s} = 240$  GeV, where two jets are clustered in the events. Only taus that are matched in angular position to the true ones are considered.

we also compare different approaches to obtain its mass. First of all, the invariant mass of the tau pair is calculated using the collinear approximation [32]. Then, the mass of the system recoiling against the tau lepton pair is extracted from the momenta of the decay products of the  $Z$  and the total energy-momentum conservation. Finally, we compare them to the invariant mass of the visible decay products of the taus. From Figure 3, the visible mass of the two taus carries the least amount of information, given the missing energy of the neutrinos. The collinear and recoil masses are capable of identifying the Higgs boson precisely, with the latter having an advantage shown by the very narrow peak.

#### 4. Cross-section at $\sqrt{s}=240$ and 365 GeV

From the discussion in Sec. 3, we choose to proceed in this analysis with the ParticleNet tau reconstruction, considering that we do not exploit the decay mode information.

*BDT classifier.* A boosted decision tree (BDT) classifier is trained in each signal category and at the different energies to focus on the specific kinematics, to enhance the signal-to-background separation compared to a traditional cut-based event selection. The BDT features include

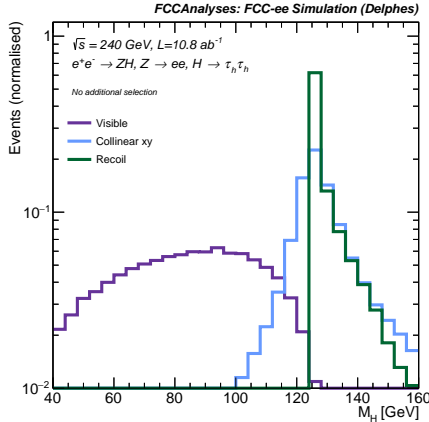


Figure 3: Comparison of different methods of reconstructing the Higgs boson mass for events where  $Z \rightarrow ee$  and  $H \rightarrow \tau_h \tau_h$ . The events have been normalized to their sum and use exclusive jets with  $n_{jets} = 2$  with the ParticleNet tau reconstruction.

the di-tau  $\Delta\phi$ ,  $\Delta\eta$ ,  $\Delta R$ , missing four-momentum, reconstructed Z and Higgs boson four-momentum,  $M_{recoil}$  and  $M_{collinear}$  where available. Each BDT has a size of 200 trees and a depth of two. We do not exclude the training set in the final analysis, as we do not observe over-training. For  $Z \rightarrow qq$  and  $Z \rightarrow \ell\ell$ , the BDTs are trained and then applied to events with  $100 < M_{collinear} < 150$  GeV for both energies, while for  $Z \rightarrow \nu\nu$  the events have  $E_{miss} > 100$  GeV. At higher energy, a sizable contribution in the  $\nu\nu\tau\tau$  final state comes from the VBF channel, so a multi-class BDT is used to separate the two signatures, with the major differences being found in the missing transverse momentum and missing mass, with the initial selection of  $E_{miss} > 180$  GeV. Figure 4 shows the BDT score distributions of the most sensitive channels in each separate energy and process.

*Results.* The cross-section measurement is extracted with the CMS Combine tool [33], analyzing the discriminating variables from the objects reconstructed in the detector simulation in a shape-based analysis. The maximum likelihood fit is performed using the BDT score distribution of each signal and background event, with four times as many bins as shown in the previous plots. We consider a log-normal uncertainty of 1% on the cross-section of the background processes  $e^+e^- \rightarrow ZZ$ ,  $e^+e^- \rightarrow WW$ , Drell-Yan, ZH, and photon-induced processes. Statistical uncertainty from the limited number of simulated events is not considered, as it does not significantly affect the result. Table 3 shows the results for the combination of each final state in the respective energies.

To extract the relative precision on  $\kappa_\tau$ , we consider the relations [15, 16]:

$$\sigma_{ZH} \times \mathcal{B}(H \rightarrow \tau\tau) \propto \frac{\kappa_\tau^2 \kappa_Z^2}{\Gamma_H},$$

$$\sigma_{\nu_e \nu_e H} \times \mathcal{B}(H \rightarrow \tau\tau) \propto \frac{\kappa_\tau^2 \kappa_W^2}{\Gamma_H},$$

$\sqrt{s}$	240 GeV	365 GeV	240+365 GeV
$\mathcal{L}$	10.8 ab $^{-1}$	3 ab $^{-1}$	13.8 ab $^{-1}$
ZH	ZH	VBF	ZH
$H \rightarrow \tau\tau$	$\pm 0.57\%$	$\pm 1.17\%$	$\pm 8.48\%$
			$\pm 0.51\%$

Table 3: The second and third columns show the relative uncertainty on  $\sigma_{ZH} \times \mathcal{B}(H \rightarrow \tau\tau)$ , while the last column refers to  $\sigma_{\nu_e \nu_e H} \times \mathcal{B}(H \rightarrow \tau\tau)$ . These values are extracted by considering the ParticleNet tau reconstruction with exclusive jet clustering and a BDT event discrimination.

where  $\Gamma_H$  is the width of the Higgs boson and  $\kappa_Z$  and  $\kappa_W$  are the coupling modifiers of the ZZH and WWH vertices. At the FCC-ee, the relative precision on these values is expected to be around  $\delta\kappa_Z = 0.1\%$ ,  $\delta\kappa_W = 0.29\%$ , and  $\delta\Gamma_H = 0.78\%$  [7]. Given this, we expect the relative precision on  $\delta\kappa_\tau = 0.47\%$  from the ZH production mode, while the VBF channel gives a worse result since it's limited by the higher background contribution.

## 5. Conclusions

In this document, we have presented a first analysis of  $H \rightarrow \tau\tau$  cross-section uncertainty in ZH events at  $\sqrt{s} = 240$  GeV and ZH and VBF events at  $\sqrt{s} = 365$  GeV for the  $e^+e^-$  Future Circular Collider (FCC-ee). In particular, the relative uncertainty expected at FCC-ee for  $\sigma_{ZH} \times \mathcal{B}(H \rightarrow \tau\tau)$  and  $\sigma_{\nu_e \nu_e H} \times \mathcal{B}(H \rightarrow \tau\tau)$  is obtained with a fast simulation of the IDEA detector concept, including all relevant background events and Z decay modes. We have also developed an algorithm to reconstruct hadronic tau decays that has been compared to a ParticleNet algorithm trained to recognize the jet flavor. Finally, a BDT classifier is employed to get higher discriminating power between signal and background.

The results of this study demonstrate that the FCC-ee could reach sub-percent precision of  $H \rightarrow \tau\tau$  cross-section in the ZH production, significantly improving the current measurement by orders of magnitude, also considering the interpretation in the  $\kappa$  framework. In contrast, in the VBF channel, the gain with respect to the LHC is less pronounced due to the lower expected number of events. Nonetheless, this illustrates how a future specialized Higgs factory can provide valuable insights into the Higgs sector.

## Acknowledgements

The work of S.G., M.K., and M.P. is supported by the Alexander von Humboldt-Stiftung. The work of M.C. is supported by grants PID2021-122134NB-C21 and CNS2023-144781 funded by MICIU/AEI /10.13039/501100011033 and FEDER,UE and European Union NextGenerationEU/PRTR.

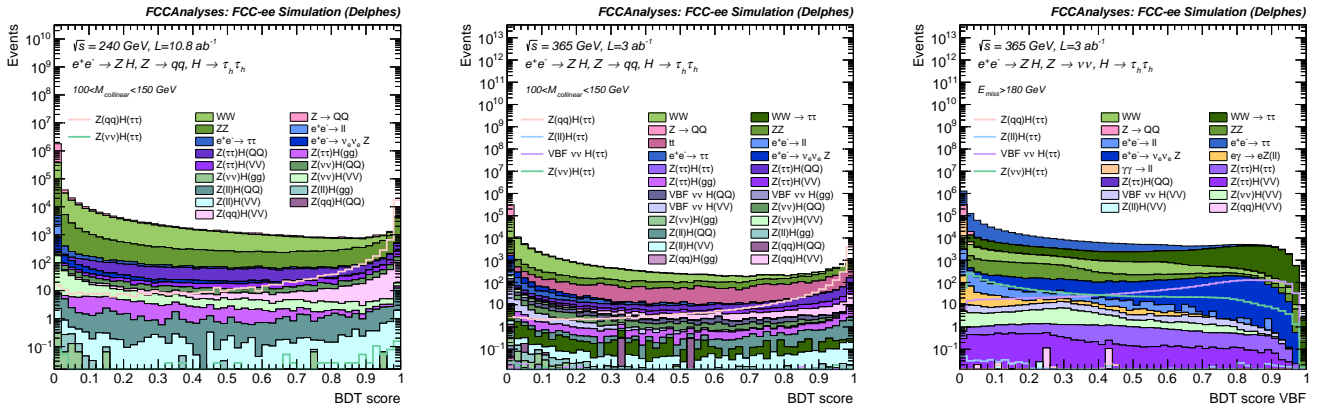


Figure 4: On the left: BDT score distribution for  $Z \rightarrow qq, H \rightarrow \tau_h \tau_h$  at  $\sqrt{s} = 240$  GeV. On the center: BDT score distribution for  $Z \rightarrow qq, H \rightarrow \tau_h \tau_h$  at  $\sqrt{s} = 365$  GeV. On the right: BDT score distribution for VBF  $H \rightarrow \tau_h \tau_h$  at  $\sqrt{s} = 365$  GeV.

## References

- [1] G. Aad, et al., Measurements of the Higgs boson production and decay rates and constraints on its couplings from a combined ATLAS and CMS analysis of the LHC pp collision data at  $\sqrt{s} = 7$  and 8 TeV, *JHEP* 08 (2016) 045. [arXiv:1606.02266](https://arxiv.org/abs/1606.02266), doi:10.1007/JHEP08(2016)045.
- [2] A. M. Sirunyan, et al., Observation of the Higgs boson decay to a pair of  $\tau$  leptons with the CMS detector, *Phys. Lett. B* 779 (2018) 283–316. [arXiv:1708.00373](https://arxiv.org/abs/1708.00373), doi:10.1016/j.physletb.2018.02.004.
- [3] J. Altmann, et al., ECFA Higgs, electroweak, and top Factory Study, Vol. 5/2025 of CERN Yellow Reports: Monographs, 2025. [arXiv:2506.15390](https://arxiv.org/abs/2506.15390), doi:10.23731/CYRM-2025-005.
- [4] G. Arduini, F. Bordry, R. Brinkmann, P. Burrows, K. Desch, S. Farrington, F. Gianotti, K. Hanagaki, N. Holtkamp, J. Keintzel, B. Kilmister, T. Lesiak, L. Rivkin, F. Sabatié, M. Tuts, A. Zoccoli, Assessment of large-scale accelerator projects at CERN - Report of ESG WG2a, Tech. rep., Geneva (2025). URL <https://cds.cern.ch/record/2947728>
- [5] J. de Blas, et al., Physics Briefing Book: Input for the 2026 update of the European Strategy for Particle Physics (11 2025). [arXiv:2511.03883](https://arxiv.org/abs/2511.03883), doi:10.17181/CERN.35CH.202P.
- [6] A. Abada, et al., FCC-ee: The Lepton Collider: Future Circular Collider Conceptual Design Report Volume 2, *Eur. Phys. J. ST* 228 (2) (2019) 261–623. doi:10.1140/epjst/e2019-900045-4.
- [7] M. Benedikt, et al., Future Circular Collider Feasibility Study Report: Volume 1, Physics, Experiments, Detectors (4 2025). [arXiv:2505.00272](https://arxiv.org/abs/2505.00272).
- [8] A. Abada, et al., FCC Physics Opportunities: Future Circular Collider Conceptual Design Report Volume 1, *Eur. Phys. J. C* 79 (6) (2019) 474. doi:10.1140/epjc/s10052-019-6904-3.
- [9] M. Benedikt, et al., Future Circular Collider Feasibility Study Report: Volume 2, Accelerators, Technical Infrastructure and Safety (4 2025). [arXiv:2505.00274](https://arxiv.org/abs/2505.00274), doi:10.1140/epjs/s11734-025-01967-4.
- [10] Prospects in electroweak, Higgs and Top physics at FCC (3 2025). doi:10.17181/n78xk-qcv56.
- [11] A. Tumasyan, et al., A portrait of the Higgs boson by the CMS experiment ten years after the discovery., *Nature* 607 (7917) (2022) 60–68, [Erratum: *Nature* 623, (2023)]. [arXiv:2207.00043](https://arxiv.org/abs/2207.00043), doi:10.1038/s41586-022-04892-x.
- [12] G. Aad, et al., A detailed map of Higgs boson interactions by the ATLAS experiment ten years after the discovery, *Nature* 607 (7917) (2022) 52–59, [Erratum: *Nature* 612, E24 (2022)]. [arXiv:2207.00092](https://arxiv.org/abs/2207.00092), doi:10.1038/s41586-022-04893-w.
- [13] M. Cepeda, et al., Report from Working Group 2: Higgs Physics at the HL-LHC and HE-LHC, CERN Yellow Rep. Monogr. 7 (2019) 221–584. [arXiv:1902.00134](https://arxiv.org/abs/1902.00134), doi:10.23731/CYRM-2019-007.221.
- [14] Projection of  $H \rightarrow \tau\tau$  cross-section measurement results to the HL-LHC, Tech. rep. (2022).
- [15] A. David, A. Denner, M. Duehrssen, M. Grazzini, C. Grojean, G. Passarino, M. Schumacher, M. Spira, G. Weiglein, M. Zanetti, LHC HXSWG interim recommendations to explore the coupling structure of a Higgs-like particle (9 2012). [arXiv:1209.0040](https://arxiv.org/abs/1209.0040).
- [16] J. R. Andersen, et al., Handbook of LHC Higgs Cross Sections: 3. Higgs Properties (7 2013). [arXiv:1307.1347](https://arxiv.org/abs/1307.1347), doi:10.5170/CERN-2013-004.

[17] G. Aad, et al., Highlights of the HL-LHC physics projections by ATLAS and CMS (4 2025). [arXiv:2504.00672](https://arxiv.org/abs/2504.00672).

[18] I. Adachi, et al., Measurement of the  $\tau$ -lepton mass with the Belle II experiment, Phys. Rev. D 108 (3) (2023) 032006. [arXiv:2305.19116](https://arxiv.org/abs/2305.19116), doi:10.1103/PhysRevD.108.032006.

[19] A. Lusiani, Tau physics prospects at fcc-ee. (2024). doi:<https://doi.org/10.17181/57pxj-6xd43>.

[20] G. Wilkinson, S. Monteil, J. F. Kamenik, A. Lusiani, Prospects in flavour physics at the fcc (Mar. 2025). doi:10.17181/jnzpp-1fw39. URL <https://doi.org/10.17181/jnzpp-1fw39>

[21] W. Kilian, T. Ohl, J. Reuter, WHIZARD: Simulating Multi-Particle Processes at LHC and ILC, Eur. Phys. J. C 71 (2011) 1742. [arXiv:0708.4233](https://arxiv.org/abs/0708.4233), doi:10.1140/epjc/s10052-011-1742-y.

[22] M. Moretti, T. Ohl, J. Reuter, O'Mega: An Optimizing matrix element generator (2001) 1981–2009 [arXiv:hep-ph/0102195](https://arxiv.org/abs/hep-ph/0102195).

[23] T. Sjostrand, S. Mrenna, P. Z. Skands, PYTHIA 6.4 Physics and Manual, JHEP 05 (2006) 026. [arXiv:hep-ph/0603175](https://arxiv.org/abs/hep-ph/0603175), doi:10.1088/1126-6708/2006/05/026.

[24] C. Bierlich, et al., A comprehensive guide to the physics and usage of PYTHIA 8.3, SciPost Phys. Codeb. 2022 (2022) 8. [arXiv:2203.11601](https://arxiv.org/abs/2203.11601), doi:10.21468/SciPostPhysCodeb.8.

[25] M. Abbrescia, et al., The IDEA detector concept for FCC-ee (2 2025). [arXiv:2502.21223](https://arxiv.org/abs/2502.21223).

[26] J. de Favereau, C. Delaere, P. Demin, A. Giannanco, V. Lemaître, A. Mertens, M. Selvaggi, DELPHES 3, A modular framework for fast simulation of a generic collider experiment, JHEP 02 (2014) 057. [arXiv:1307.6346](https://arxiv.org/abs/1307.6346), doi:10.1007/JHEP02(2014)057.

[27] M. Cacciari, G. P. Salam, G. Soyez, FastJet User Manual, Eur. Phys. J. C 72 (2012) 1896. [arXiv:1111.6097](https://arxiv.org/abs/1111.6097), doi:10.1140/epjc/s10052-012-1896-2.

[28] H. Qu, L. Gouskos, ParticleNet: Jet Tagging via Particle Clouds, Phys. Rev. D 101 (5) (2020) 056019. [arXiv:1902.08570](https://arxiv.org/abs/1902.08570), doi:10.1103/PhysRevD.101.056019.

[29] F. Bedeschi, L. Gouskos, M. Selvaggi, Jet flavour tagging for future colliders with fast simulation, The European Physical Journal C 82 (7) (Jul. 2022). doi:10.1140/epjc/s10052-022-10609-1. URL <http://dx.doi.org/10.1140/epjc/s10052-022-10609-1>

[30] D. Jeans, Tau lepton reconstruction at collider experiments using impact parameters, Nucl. Instrum. Meth. A 810 (2016) 51–58. [arXiv:1507.01700](https://arxiv.org/abs/1507.01700), doi:10.1016/j.nima.2015.11.030.

[31] K. Belous, et al., Measurement of the  $\tau$ -lepton lifetime at Belle, Phys. Rev. Lett. 112 (3) (2014) 031801. [arXiv:1310.8503](https://arxiv.org/abs/1310.8503), doi:10.1103/PhysRevLett.112.031801.

[32] P. Konar, A. K. Swain, Reconstructing semi-invisible events in resonant tau pair production from higgs, Physics Letters B 757 (2016) 211–215. doi:10.1016/j.physletb.2016.03.070. URL <https://www.sciencedirect.com/science/article/pii/S0370269316300417>

[33] A. Hayrapetyan, et al., The CMS Statistical Analysis and Combination Tool: COMBINE, Submitted to Computing and Software for Big Science (4 2024). [arXiv:2404.06614](https://arxiv.org/abs/2404.06614).